中國機械工程學刊第四十一卷第一期第 11~20 頁(民國一百零九年)
Journal of the Chinese Society of Mechanical Engineers, Vol.41, No.1, pp 11~20 (2020)

The Effect of the Acetylene Gas Flow Rate and Doping with Titanium on the Mechanical and Tribological Properties of Diamond-Like Carbon

Yen-Liang Su*, Jeng-Haur Horng**, Elena Torskaya***
,Wen-Hsien Kao**** and Chang-Ching Yu*****

Keywords: DLC, Titanium, Wear, Corrosion

ABSTRACT

This study determines the mechanical and tribological properties of Diamond-Like Carbon (DLC), DLC doped titanium (DLC-Ti) and hydrogenated DLC doped titanium (DLC-CH-Ti) coatings. These coatings are deposited on a high-speed steel substrate (SKH51) using Closed Field Unbalanced Magnetron Sputtering (CFUBMS). GDS and EDX analysis shows that when acetylene flow rate is added in deposited chamber, the content of the metallic element (titanium) decreases. The surface morphology for all coatings exhibits a clustered morphology. The XPS analysis at the C1s core level shows that the C-C sp^3 ratio increases as that acetylene gas and the titanium content are added. The DLC-CH-Ti coating has the optimal mechanical and tribological properties, with a wear rate of 0.09 ($10^{-6}mm^3/Nm$) and a friction coefficient of 0.11as sliding against an Al_2O_3 ball. These results are much better than those for the other coatings. The wear rate is 194 times less than that for the substrate alone and the corrosion resistance of the coatings is better than that for the original substrate.

INTRODUCTION

The basic physical, mechanical and tribological properties of diamond-like carbon (DLC) coatings have been the subject of many studies (Bewilogua et al., 2000; Corbella et al., 2005; Hung et al., 2015; Petersen et al., 2011; Strondl, 2003; Wu and Ting, 2002).The coatings exhibit high hardness, a low coefficient of friction, high wear resistance and chemical inertness (Andersson et al., 2003; Spear and Dismukes, 1994; Kodali et al., 1997; Ronkainen et al., 1998), and they protect the opposing rubbing surface from significant wear without the use of a lubricant. This combination of properties means that DLC coatings are applicable in a variety of tribological applications, such as DLC coatings on cutting tools and micro-drills (Hsu et al., 2013).

DLC coatings are extremely common in industry meet the increasingly stringent application requirements for advanced machining, where coatings must have a low coefficient of friction and high wear resistance. Lin et al. (2014) reported that oscillating waveforms can be used to deposit DLC that has high hardness and a low wear rate. Muencivondy et al. (2014) used high-power impulse magnetron sputtering and a multi-layer composite film to deposit DLC. The adhesion、hardness and wear resistance are 1.75 times better than the normal DLC.

DLC coatings can be deposited on many materials. Bui et al. (2008) deposited Ti-DLC coatings on HNBR rubber, in order to increase the wear resistance of the rubber surface. Silva et al. (2011) deposited DLC and types of coatings to protect a glass fiber substrate.

DLC coatings exhibit a large intrinsic compressive stress. This stress causes poor adhesion at the coating-to-substrate interface (Robertson, 2002), which limits that coating's applications. A number of methods minimize this effect. If an interlayer is used between the substrate and the coating or a graded layer or multi-layered coating, this problem is mitigated (Jeon and Kim, 2007; Wei and Yen, 2007). Some modeling results also demonstrate the positive effect of intermediate layers (Goryacheva and Torskaya,

Paper Received May, 2019. Revised November, 2019. Accepted December, 2019. Author for Correspondence: Wen-Hsien Kao.

**Professor, Department of Mechanical Engineering, National Cheng Kung University, Tainan, Taiwan.*
***Professor, Department of Power Mechanical Engineering, National Formosa University, Yunlin, Taiwan*
****Professor, Ishlinsky Institute for Problems in Mechanics, Russian Academy of Sciences, Moscow, Russia*
*****Professor, Department of Automation Engineering, Chienkuo Technology University, Changhua, Taiwan.*
******Master, Department of Mechanical Engineering, National Cheng Kung University, Tainan, Taiwan.*

2016). This study deposits a metal interlayer onto the substrate and then deposits a progressive layer. The main coating is finally deposited onto the progressive layer.

Amorphous hydrogenated carbon (a-C:H) and metal that contains diamond-like carbon (Me-DLC) are used to improve the properties of DLC. The a-C:H is a type of DLC, which is deposited using a hydrocarbon gas. Gases such as methane, acetylene or benzene can be used. The a-C:H coating composite with increased hydrogen creates a carbon structure that exhibits more C-H bonding, so the carbon structure features less compressive stress. If the concentration of hydrogen is controlled, the compressive stress is reduced and there is better adhesion (Robertson, 1994).

Metal that contains diamond-like carbon (Me-DLC) is also a type of DLC coating. Alloying using carbide-forming metals results in an increase in strength because nano-sized carbide inclusions are created. If Si is added to a-C:H the stress is decreased and the friction coefficient is reduced (Oguri and Arai, 1991). The addition of a metal element has been shown to improve the properties of DLC. Ronkasinen et al. (2001) reported that Ti-DLC:H coatings exhibit excellent self-lubricating properties and have a coefficient of friction of 0.10 and demonstrated that Ti improves the performance of the DLC:H coatings (Ronkainen et al., 2001).

There are many methods of improving the properties of DLC coatings. Although the mechanical and tribological properties of DLC、a-C:H and Me-DLC have been the subject of many studies, the authors find that these types of coatings have seldom been compared. This study deposits DLC coatings on SKH51 steel substrate using CFUBMS, with titanium metal or acetylene gas, and determines the mechanical and tribological properties of the coatings.

EXPERIMENTAL DETAILS

Preparation of the Coatings

This study uses CFUBM to produce DLC coatings and other series on SKH51 disks (HRC 65) substrate. The unbalanced magnetron sputtering system contains three graphite targets and one titanium target (Target size: 300 mm x 109 mm x 10 mm). Acetylene gas was used as the hydrocarbon gas. Before deposition of the DLC coatings, the surface of the SKH51 substrates were polished with Ra= 0.08 μm, ultrasonically cleaned in acetone and bombarded with argon ions for 20 min at a bias voltage -340 V. After bombardment, a pure titanium layer was deposited to serve as an interface with the substrate. The substrate was rotated at 3 rpm, in order to increase adhesion between the substrate and the coating.

The coating experiment has two parts. Firstly, 0A and 1A titanium target currents were used to deposit DLC and DLC-Ti coatings. Acetylene gas at a flow rate of 8 sccm was then used to deposit the DLC-CH-Ti coatings. The parameters for this process (target currents、gas flow rate) were determined in previous studies by the authors (Kao et al., 2010; Kao et al., 2015). Figure 1 shows each stage of the deposition of the coating on the substrate. The deposition parameters are listed in Table 1. For DLC-CH-Ti, the substrate bias was -80V for all deposition process. For DLC and DLC-Ti, the substrate bias was -80V for the interface and the progressive layer and -40V for the main coating.

Table 1. Sputtering parameters

Stage	Code	Deposition parameters				
		Ti target current (A)	C target Current (A)	C_2H_2 flow rate (sccm)	Deposition time (min)	Fixed parameters
Interlayer		1	0	0	10	Ar flow rate: 30 sccm, rotation speed: 3 rpm,
Progressive layer		1	2	0	6	
Main coating	DLC	0	2.5	0	120	
	DLC-Ti	1	2.5	0	120	
	DLC-CH-Ti	1	2.5	8	120	

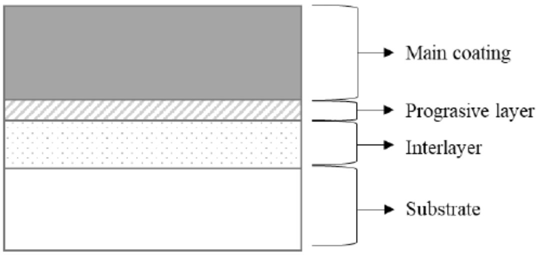

Fig. 1. The stages for the deposition of a coating on a substrate.

Characterization of Coatings

The structure of the DLC coatings was characterized using a variety of analytical techniques. Raman spectroscopy was used to determine the bonding structure of the coatings. The spectra were recorded at room temperature in backscattering geometry over a range of 1000-2000 cm^{-1}, using an Ar-ion laser (λ = 514 nm) operating at a power of 20mW. A microprobe was configured to produce a spot size of about 1 μm.-The peak intensity was calculated and the change in the position of the peak and the FWHM were used to determine the bonding structure of the coatings.

The chemical composition of the coatings was determined using glow discharge spectrometry (GDS) and the chemical bonding was analyzed using X-ray photoelectron spectroscopy (XPS) with a light source of Al Kα, operating at a wavelength of 100 μm and the bounding energy was scanned in the range, 0 to 1400 eV. The Gaussian-Lorentzian method was used to calculate the XPS spectrum, using Origin Lab software, in order to determine the chemical bonding ratio for the coatings.

Mechanical、Adhesive、Tribological、Oxidative and Anti-corrosive Properties

The mechanical and adhesive properties were respectively determined using nano-indentation and a scratch tester. The nano indenter (LBI Nanoindenter, UNAT-M, Germany) test on the surface of the coating was repeated five times, using a load of 10 mN, in order to measure the hardness and the Young's modulus. The scratch tester used a diamond cone with a diameter of 300 μm and a load that increased at a rate of 1 N per second, from 0N to 100 N, for a scratch distance of 10 mm. SEM was used to determine the point on the scratch scar at which the coating was broken, in order to determine the critical load (Lc). A critical load demonstrates better adhesion between the coating and the substrate. The tribological properties were measured using a ball-on-disk tribometer in an ambient environment. SKH51 was coated and used against the ball (uncoated Al_2O_3 ball) under a 10N load and at sliding speed of 0.3m/s for 5000 rotations. The coefficient of friction was then recorded. White light interferometry (WLI) was used to measure the wear depth and the cross sectional area of the wear. The product of the cross sectional area of the wear and the circumference of the wear trace gives the wear volume. The wear rate is calculated as: ($\text{wear rate} = \frac{\text{wear volume}}{\text{normal load} \times \text{sliding distance}}$).

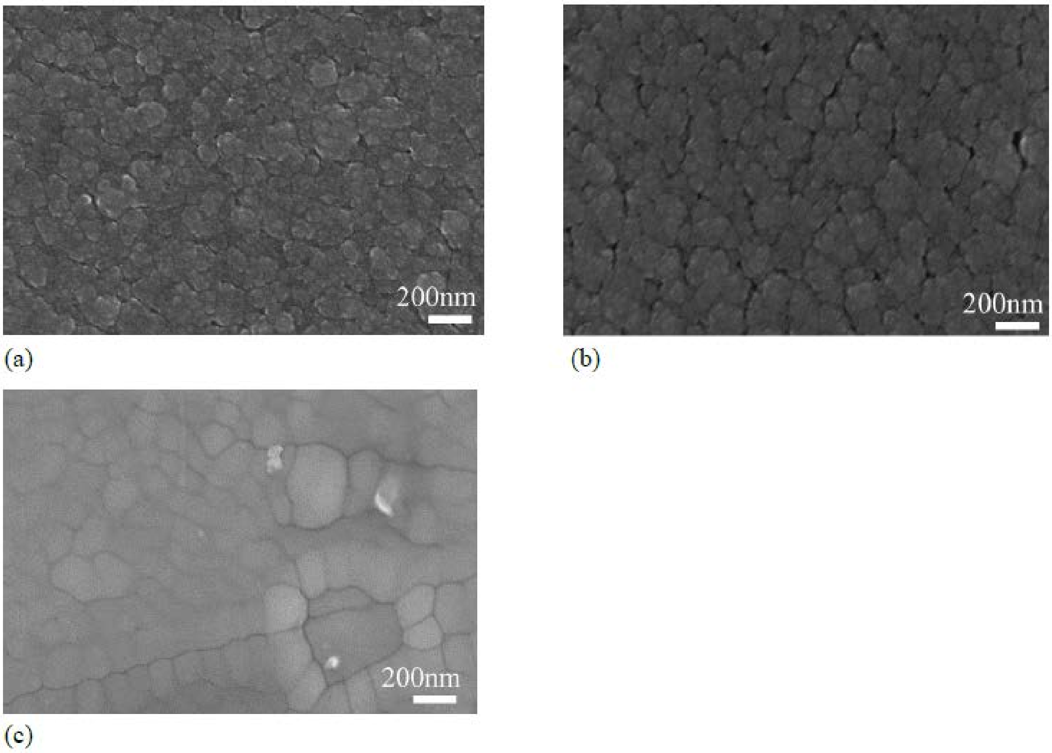

Fig. 2. The surface morphology of the coatings: (a) DLC, (b) DLC-Ti and (c) DLC-CH-Ti.

Table 2. The C1s result for X-ray photoelectron spectroscopy

Sample	C-C Sp^3(%)	C=C Sp^2(%)	C-O(%)	C-Ti(%)
DLC	11.9	85.93	2.16	-
H-DLC	18.82	75.1	6.08	-
DLC-Ti	22.85	77.63	3.77	0.1
H-DLC-Ti	25.96	72.77	6.62	0.1
DLC-CH-Ti	31.51	72.07	3.97	0.1
H-DLC-CH-Ti	17.62	75.56	9.46	0.1

“H-” means the coating after heat treatment

High temperature tests were used to determine resistance to oxidization. An electric furnace (Type FB1300) was heated to 250˚C and the coatings were baked for an hour, before they were cooled to room temperature. The heated coatings are signified by an “H-” prefix: H-DLC、H-DLC-Ti and H-DLC-CH-Ti.

The electrochemical tests were performed in 0.9 wt.% NaCl solution at room temperature, using a potentiostat (ECW-5000, Jiehan, Taiwan). The test area was 1 cm^2. The open circuit potential was measured for 60 seconds before the potentiodynamic polarization tests were initiated and the electrode potential was found to increase from −1V to 3V at a scanning rate of 1 mV/s. Tafel extrapolation was used to determine the anti-corrosion properties for all of the coatings after the tests. The surface morphology was observed using SEM.

RESULT

Structure and Chemical Composition

Figure 2 shows the surface morphology. All coatings have a clustered morphology, possibly because the energy that is used to bombard the surface is not sufficiently great, so the structure of the coatings is loose and forms this clustered morphology (Zheng et al., 2014). The plot of titanium content versus glow discharge spectrometry (GDS) shows that DLC-Ti has

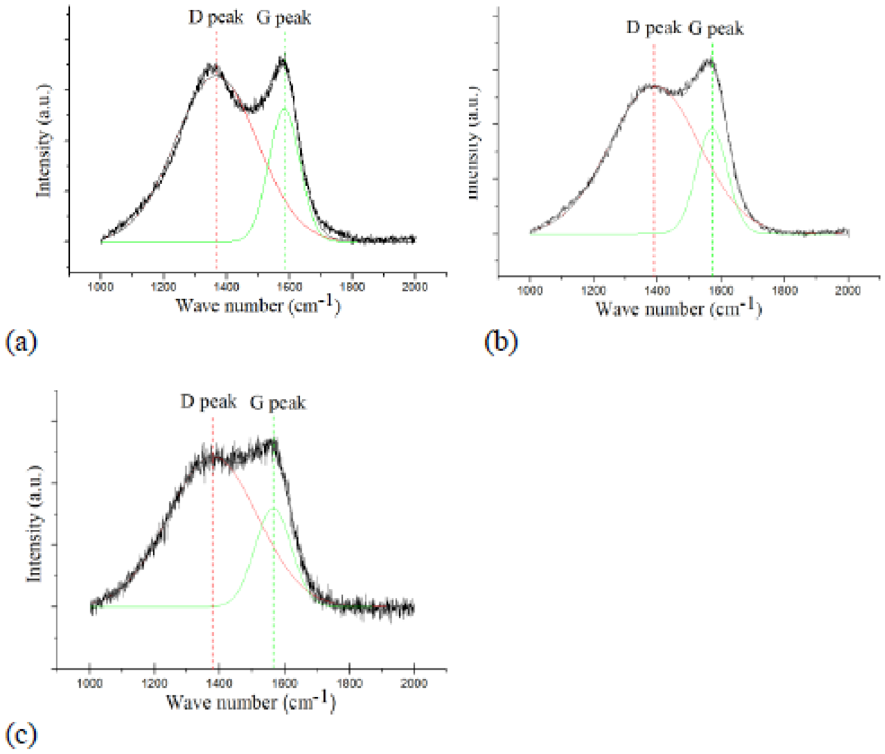

Fig. 3. Raman spectra before heat treatment: (a) DLC (b) DLC-Ti (c) DLC-CH-Ti.

Sample	D peak position(cm^{-1})	G peak position(cm^{-1})	G peak FWHM(cm^{-1})	ID/IG
DLC	1364.1	1581	117.7	1.39
H-DLC	1390.3	1584.8	105.2	1.06
DLC-Ti	1391.3	1571.9	114.9	1.39
H-DLC-Ti	1391.1	1572.7	113.9	1.44
DLC-CH-Ti	1395.5	1571.1	96.1	1.24
H-DLC-CH-Ti	1390.9	1574.2	123.8	1.48

“H-” means the coating after heat treatment

Table 3. Results for the Raman spectra before and after heat treatment

the highest titanium content, at 16 at %. The DLC-CH-Ti coating has a titanium content of only about 5 at %. The titanium content decreases as the acetylene gas was added into deposited chamber, because the target surface is strongly bombarded with Ar+ ions, so more Ti atoms are sputtered when the only Ar flow, which leads to an increase in Ti concentration. When the C_2H_2 flow is added into the chamber, the target surface is covered by carbon from ionized C_2H_2, which causes a decrease in Ti concentration (Cui, 2012).

Table 2 shows the results of X-ray photoelectron spectroscopy (XPS) analysis. The respective values for C 1s is 280-295 eV (Cheng and Zheng, 2007). XPS was used to analyze the ratio of coating bonding and the results were compared with those for the mechanical properties. The C 1s wave consists of three waves: the C=C sp^2 peak (284.5 ± 0.1eV) 、the C-C sp^3 peak (285.3 ± 0.2 eV) and the C-O peak (288.5 ± 0.2 eV). Robertson (2002) showed that diamond-like carbon is a metastable form of amorphous carbon with significant C-C sp^3 bonding. A DLC coating with more C-C sp^3 bonding demonstrates significantly improved mechanical and tribological properties. Table 2 shows that the C-C sp^3 ratio is increased after doping with metal and the use of acetylene. The DLC-CH-Ti coating that contains metal and for which acetylene is used has the highest value for the C-C sp^3 bonding percentage.

After heat treatment, the DLC coating and the DLC-Ti coating both exhibit slightly reduced C=C sp^2 bonding and slightly increased C-C sp^3 bonding. C-O bonding, which represents the extent to which the coating is oxidized, is increased. C-C sp^3 bonding in the DLC-CH-Ti coating is significantly reduced from 31.51% to 17.62%, which demonstrates that the diamond structure of DLC-CH-Ti is significantly reduced. The C-O bonding for the DLC-CH-Ti coating is increased from 3.97% to 9.46%. Heat-treated DLC-CH-Ti after heat treatment exhibits the highest degree of oxidation of all of the coatings.

The Raman spectra before heat treatment are shown in Figure 3. The D peak and the G peak are evident in the figure and the two peak positions are shown in Table 3. In a typical DLC structure, the two peaks are located at approximately 1350 cm^{-1}and 1580 cm^{-1}, respectively (Ferrari and Robertson, 2000). The wave number for the D peak for all types of coatings are shifted to a higher position than the original position (1350 cm^{-1}), which demonstrates that these coatings have a disordered carbon structure (Capano et al., 1996). The G peaks for DLC-Ti and DLC-CH-Ti are shifted to a lower wave number, which demonstrates that there is an increase in C-C sp^3 bonding (Bai and Jiang, 1999; Zhu et al., 1991). This result is in agreement with the results for XPS analysis, which show that DLC-Ti and DLC-CH-Ti exhibit more C-C sp^3 bonding than DLC.

Table 3 shows the Raman spectra before and after heat treatment. The ID/IG ratio for DLC-Ti and DLC-CH-Ti is greater after heat treatment, so the coatings may have more defects after heat treatment. The FWHM for the G peak for DLC-CH-Ti increases from 96.1 to 123.8, but the other coatings exhibit a decrease. The FWHM for the G peak for DLC decreases from 117.7 to 105.2 and the FWHM for the G peak for DLC-Ti decreases from 114.9 to 113.9. These results are similar to those for other studies (Tallant et al., 1995; Yang et al., 2003).The increase in the FWHM is indicative of graphitization. The graphitization process can reduce the hardness of the

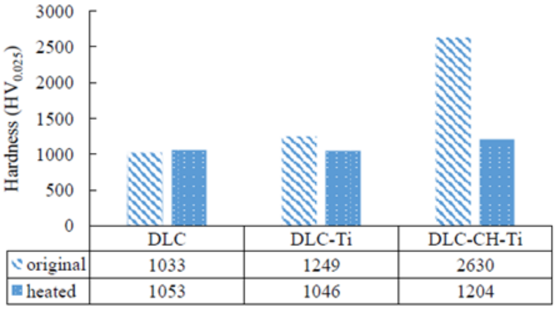

Fig. 4. Hardness values before and after heat treatment

Table 4. Results for the mechanical properties, surface roughness, critical load and coating thickness.

	Hardness (GPa)	Elastic modulus (GPa)	Surface roughness Ra (nm)	Critical load (N)	Coating thickness (μm)
DLC	13.3	181.3	37	83	1.43
DLC-Ti	12.3	155.6	25	73	1.9
DLC-CH-Ti	25.9	278.7	45	97	1.41

coating and result in poor wear resistance at high temperatures (Ni et al., 2006). After heat treatment, the XPS and Raman analysis shows that the diamond structure of DLC-CH-Ti coating is reduced and the degree of oxidation is the greatest.

Properties of the Coatings

The thickness、the hardness and the adhesive properties of the coatings are shown in Table 4. The results for nano-hardness show that the DLC-CH-Ti coating has the highest hardness, at 25.9 GPa, so the DLC-CH-Ti coating has the highest wear resistance. In terms of adhesion, all the coatings demonstrate a critical load of more than 70 N in the scratch test. DLC-CH-Ti exhibits excellent adhesion, with a load of 97 N. It is shown that the DLC-CH-Ti coating has the highest hardness and adheres better than other coatings.

The results for hardness before and after heat treatment are shown in Figure 4. The hardness of DLC-Ti and DLC-CH-Ti decreases after heat treatment and the hardness of DLC slightly increases. The hardness of DLC-CH-Ti coatings decreases more than a thousand-fold after heat treatment. The XPS and Raman results (as shown in Table 2 and Table 3, respectively) show that there is significantly less C-C sp^3 bonding in the DLC-CH-Ti coating after heat treatment, with a decrease from 31.51 % to 17.62%. There is more C-O bonding (from 3.97% to 9.46%) and it exhibits the highest degree of oxidation. The XPS results show that the DLC coatings exhibit a slight increase in C-C sp^3 bonding (from 11.9 %to 18.82%) and Raman analysis shows that the ID/IG

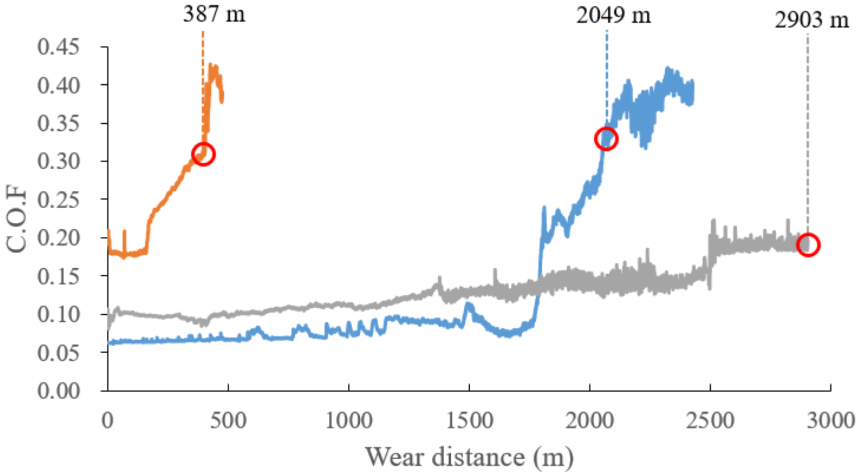

Fig. 5. The coefficient of friction (C.O.F) for the 350m wear test: (a) DLC, (b) DLC-Ti, (c) DLC-CH-Ti and (d) uncoated high speed steel.

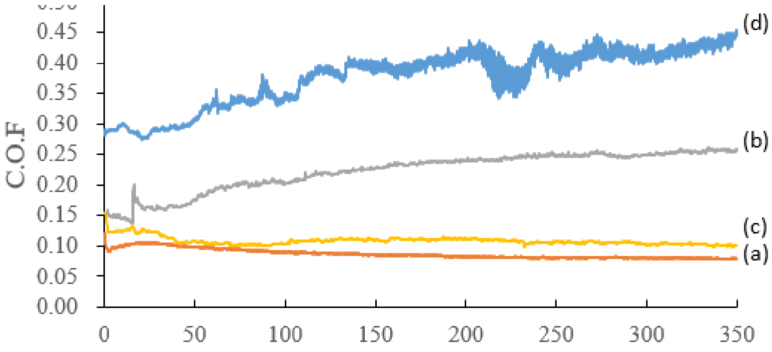

Fig. 6. Wear life: (a) DLC, (b) DLC-Ti and (c) DLC-CH-Ti.

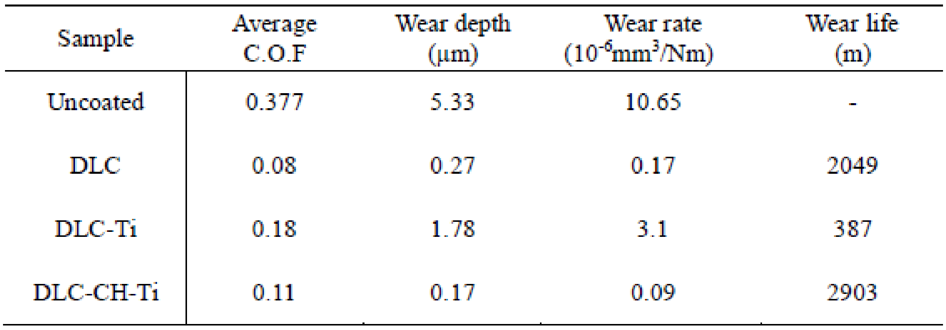

Sample	Average C.O.F	Wear depth (μm)	Wear rate ($10^{-6}mm^3/Nm$)	Wear life (m)
Uncoated	0.377	5.33	10.65	-
DLC	0.08	0.27	0.17	2049
DLC-Ti	0.18	1.78	3.1	387
DLC-CH-Ti	0.11	0.17	0.09	2903

Table 5. Results for the tribological properties

ratio decreases from 1.39 to 1.06. It is seen that the hardness of DLC increases slightly and the hardness of DLC-CH-Ti is greatly decreased.

Tribological Properties

The results for wear are listed in Table 5. The DLC-CH-Ti exhibits the shallowest wear depth, the lowest wear rate and the longest wear life, because it has the highest hardness and critical load values (as shown in Table 4). It has the best tribological properties of all of the coatings. Figure 5 shows the coefficient of friction during the wear test. The DLC-CH-Ti and DLC coatings exhibit a low and stable coefficient of friction (C.O.F) throughout the wear test. The DLC-Ti coating exhibits a high C.O.F, which gradually increases form 24 m to350 m. The final C.O.F value is similar to that for the original substrate.

The results for the wear life test for all coatings are shown in Figure 6. The wear life is determined using the value for the C.O.F at which it suddenly increases and begins to fluctuate, or it is seen that the wear on the substrate is macroscopic. The DLC

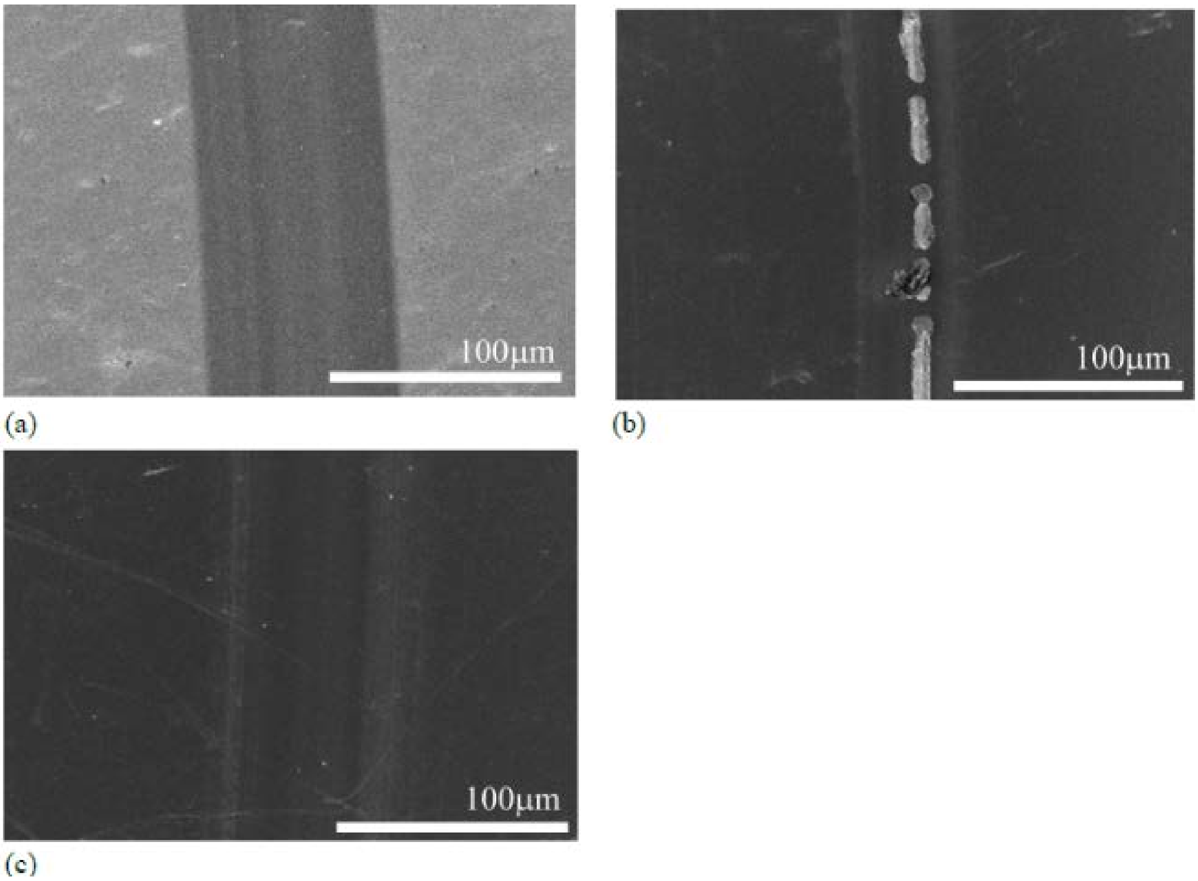

Fig. 7. The surface morphology of the coatings after the 350 m wear test :(a) DLC, (b) DLC-Ti and (c) DLC-CH-Ti.

coating has a wear life of about 2049 m. The DLC-CH-Ti coatings have the longest wear life, at close to 3000 meters. The DLC-Ti coating has the shortest wear life, at 387 meters, because it has a low hardness and adheres poorly.

Figure 7 shows the surface morphology of the coatings after a 350 m wear test. A part of the DLC-Ti coating flakes from the substrate, which demonstrates that the DLC-Ti coating has poor wear resistance. The DLC and DLC-CH-Ti coatings do not flake from the substrate, which demonstrates better wear resistance.

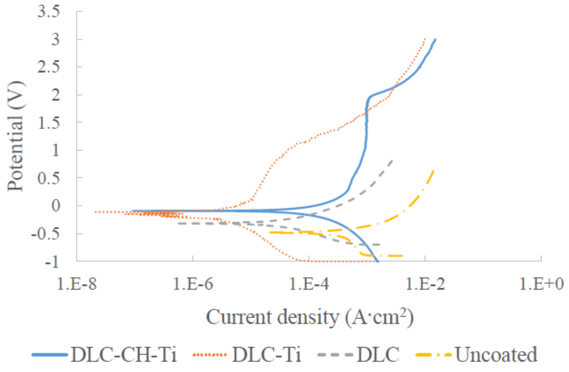

Fig. 8. Potentiodynamic polarization curves for all specimens.

Corrosion Resistance

The resistance to corrosion properties was determined by studying the anodic polarization behavior. The polarization curves are shown in Figure 8. The corrosion current density and the corrosion potential are calculated using the Tafel plot and the results are listed in Table 6. It is seen that samples on the potentiodynamic polarization curve that have a lower corrosion current density and higher corrosion potential are more resistant to corrosion. Resistance to corrosion is principally a factor of the corrosion current density. All of the coated samples feature a much lower corrosion current density than the corresponding uncoated sample, which demonstrates that the coatings increase resistance to corrosion. The corrosion current density ranking for the coatings decreases in the order: DLC-Ti > DLC-CH-Ti > DLC. The lowest corrosion current density for a coating is 0.23E-05 A/cm^{-2}, which is 130.8 times less than that for an uncoated sample.

Table 6. Results for resistance to corrosion

Sample	Corrosion voltage (V)	Corrosion current (10^{-5}A/cm^2)
Uncoated	-0.477	30.09
DLC	-0.326	3.61
DLC-Ti	-0.164	0.23
DLC-CH-Ti	-0.093	2.17

SEM surface micrographs for DLC and DLC-Ti coatings after corrosion are shown in Figure 9. The DLC-Ti coating exhibits less pitting than its DLC counterpart and retains a more intact morphology. The DLC-Ti coating has the lowest corrosion current density so it demonstrates the best resistance to corrosion resistance of all of the coatings, because it has the highest titanium content so a titanium oxide layer is formed during the test (Kuptsov et al., 2013).

SUMMARY

This study presents a comprehensive analysis of a variety of DLC coatings that are doped with Ti metal or with hydrogen and Ti metal. The experiment results show the different properties of the three types of coatings as follow:

1. When the acetylene gas is added into chamber, the target surface is covered by carbon from ionized C_2H_2, which results in a decrease in the Ti concentration of DLC-CH-Ti.
2. The C-C sp^3 ratio increases when the acetylene flow is added in the chamber, but the there is less C-C sp^3 bonding in the DLC-CH-Ti coating and an increase in C-O bonding after heat treatment.

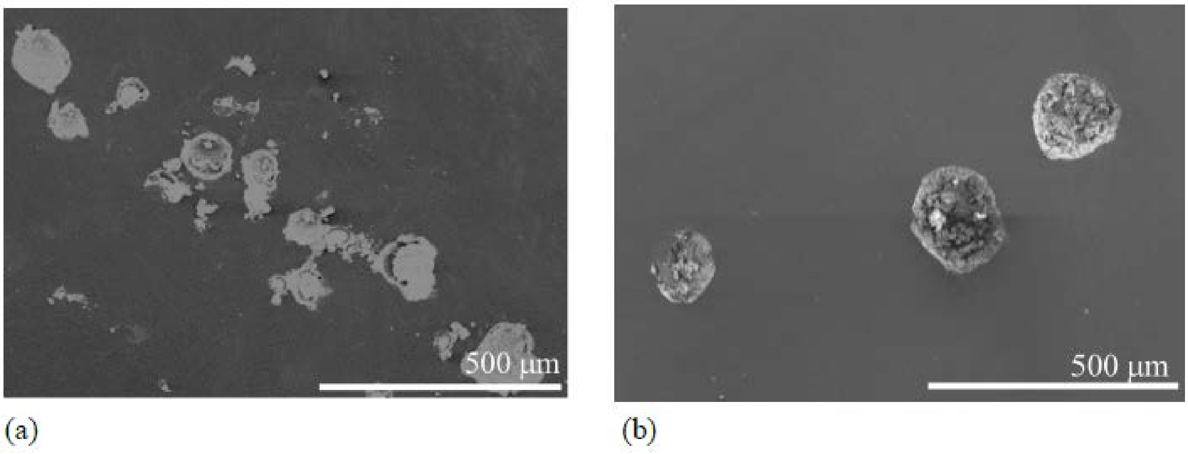

Fig. 9. SEM surface micrographs after corrosion: (a) DLC and (b) DLC-Ti

3. The Raman spectra show that the ID/IG ratio for the DLC-Ti and DLC-CH-Ti coatings increases and the ID/IG ratio for the DLC coating decreases after heat treatment. This demonstrates that the DLC-Ti and DLC-CH-Ti coatings have more defects. After heat treatment, the structure of the DLC-CH-Ti coating has more defects than other coatings.
4. The DLC-CH-Ti coating performs best in the wear tests, with a wear rate of 0.09 ($10^{-6}mm^3/Nm$) and a coefficient of friction of 0.11 against an Al_2O_3 ball. The wear rate for the coating is 194 times less than that for the substrate.
5. The coatings' resistance to corrosion is better than that for a bare substrate. DLC-Ti coatings have the lowest current density and exhibit the best resistance to corrosion.
6. In the future, these coatings can be deposited on micro-drills. After high speed drilling test, micro-drills will be analyzed and decided their life. Thereby, it can be confirm about whether these coatings are suitable for applying on industry production or not.

ACKNOWLEDGEMENT

The authors gratefully acknowledge the financial support provided to this study by the Ministry of Science and Technology of Taiwan under Contract No. MOST106-2221-E-006-093

REFERENCES

Andersson, J., Erck, R.A., & Erdemir, A. "Friction of diamond-like carbon films in different atmospheres". *Wear*, Vol. 254, pp. 1070-1075 (2003).

Bai, H.L., & Jiang, E.Y. "Improvement of the thermal stability of amorphous carbon films by incorporation of nitrogen". *Thin Solid Films*, Vol. 353, pp. 157-165 (1999).

Bewilogua, K., ooper, C.V., & Specht, C. "Effect of target material on deposition and properties of metal-containing DLC (Me-DLC)". *Surface and Coatings Technology*, Vol. 127, pp. 223-231 (2000).

Bui, X.L., Pei, Y.T., & Hosson, J.T.M.D. "Magnetron reactively sputtered Ti-DLC coatings on HNBR rubber: The influence of substrate bias". *Surface and Coatings Technology*, Vol. 202, pp. 4939-4944 (2008).

Capano, M.A., Mcdevitt, N.T., & Singh, R.K. "Characterization of amorphous carbon thin films". *Journal of Vacuum Science & Technology A*, Vol. 14, pp. 431-435 (1996).

Cheng, Y., & Zheng, Y.F. "Characterization of TiN, TiC and TiCN coatings on Ti–50.6 at.% Ni alloy deposited by PIII and deposition technique". *Surface and Coatings Technology*, Vol. 201, pp. 4909-4912 (2007).

Corbella, C., Oncins, G., & Gómez, M.A. "Structure of diamond-like carbon films containing transition metals deposited by reactive magnetron sputtering". *Diamond and Related Materials*, Vol. 14, pp.1103-1107 (2005).

Cui, J., Qiang, L., & Zhang, B. "Mechanical and tribological properties of Ti-DLC films with different Ti content by magnetron sputtering technique". *Applied Surface Science*, Vol. 258, pp. 5025-5030 (2012).

Ferrari, A.C., & Robertson, J. "Interpretation of Raman spectra of disordered and amorphous carbon". *Phys. Rev. B*, Vol. 61, pp.14095-14107 (2000).

Goryacheva, I.G., & Torskaya, E.V. "Modeling the influence of the coating deposition technology on the contact interaction characteristics". *Mechanics of Solids*, Vol. 51(5), pp. 550-556 (2016).

Hsu J.S., Tzeng S.S., Kuo C.M., & Wu Y.J. "Correlations between deposition parameters, mechanical properties, and microstructure for diamond-like carbon films synthesized by RF-PECVD". *Journal of the Chinese Institute of Engineers*, Vol 36, pp.157-163 (2013).

Hung C.P., Wu S.M., & Wang S.H. "Effects of DLC coating on relaxing surface residual stress of the weld in titanium-bearing high-strength steel". *Journal of the Chinese Institute of Engineers*, Vol. 38, pp. 645-652 (2015).

Information on: https://worldwide.espacenet.com/publicationDetails/biblio?CC=CN&NR= 104213076A&KC=A&FT=D

Jeon, Y., Park, Y.S., & Kim, H.J. "Tribological Properties of Ultrathin DLC Films with and without Metal Interlayers". *Journal of the Korean Physical Society*, Vol. 51, pp.1124-1128 (2007).

Kao, W.H., Su, Y.L., & Horng, J.H. "Improved tribological, electrochemical and biocompatibility properties of Ti6Al4V alloy by gas-nitriding and Ti–C:H coating". *Surface and Coatings Technology*, Vol. 283, pp. 70-79 (2015).

Kao, W.H., Su, Y.L., & Yao, S.H. "Optimizing the tribological properties and high-speed drilling performance of a-C:H coatings via nitrogen addition". *Surface and Coatings Technology*, Vol. 204, pp. 1277-1287 (2010).

Kodali, P., Walter, K.C., & Nastasi, M. "Investigation of mechanical and tribological properties of amorphous diamond-like carbon coatings". *Tribology International*, Vol. 30, pp. 591-598 (1997).

Kuptsov, K.A., Kiryukhantsev-Korneev, P.V., & Sheveyko, A.N. "Comparative study of electrochemical and impact wear behavior of TiCN, TiSiCN, TiCrSiCN, and TiAlSiCN coatings”. *Surface and Coatings Technology*, Vol. 216, pp. 273-281 (2013).

Lin, J., Sproul, W.D., & Wei, R. “Diamond like carbon films deposited by HiPIMS using oscillatory voltage pulses”. *Surface and Coatings Technology*, Vol. 258, pp. 1212-1222 (2014).

Muencivondy, “Method and equipment for preparing ultra-hard DLC coatings through PVD and HIPIMS”; CN104213076A, European patent (2014).

Ni, W., Cheng, Y.T., & Weiner, A.M. “Tribological behavior of diamond-like-carbon (DLC) coatings against aluminum alloys at elevated temperatures”. *Surface and Coatings Technology*, Vol. 201, pp. 3229-3234 (2006).

Oguri, K., & Arai, T. “Tribological properties and characterization of diamond-like carbon coatings with silicon prepared by plasma-assisted chemical vapour deposition”. *Surface and Coatings Technology*, Vol. 47, pp. 710-721 (1991).

Petersen, M., Heckmann, U., & Bandorf, R. “Me-DLC films as material for highly sensitive temperature compensated strain gauges”. *Diamond and Related Materials*, Vol. 20, pp. 814-818 (2011).

Robertson, J. “Diamond-like amorphous carbon”. *Materials Science and Engineering: R: Reports*, Vol. 129, pp.129-281 (2002).

Robertson, J. “The deposition mechanism of diamond-like a-C and a-C: H”. *Diamond and Related Materials*, Vol. 3, pp. 361-368 (1994).

Ronkainen, H., Varjus, S., & Holmberg, K. “Friction and wear properties in dry, water- and oil-lubricated DLC against alumina and DLC against steel contacts”. *Wear*, Vol. 222, pp.120-128 (1998).

Ronkainen, H., Varjus, S., & Holmberg, K. “Tribological performance of different DLC coatings in water-lubricated conditions”. *Wear*, Vol. 249, pp. 267-271 (2001).

Silva, F.J.G., Martinho, R.P., & Alexandre, R.J.D. “Increasing the wear resistance of molds for injection of glass fiber reinforced plastics”. *Wear*, Vol. 271, pp. 2494-2499 (2011).

Spear, K.E., & Dismukes J.P., Synthetic Diamond: Emerging CVD Science and Technology, chapter 5, Development and status of diamond-like carbon, John Wiley and Sons, New York, N.Y., pp. 91-144 (1994).

Strondl, C., Carvalho, N.M., & M De Hosson, J.T. “Investigation on the formation of tungsten carbide in tungsten-containing diamond like carbon coatings”. *Surface and Coatings Technology*, Vol. 162, pp. 288-293 (2003).

Tallant, D.R., Parmeter, J.E., & Siegal, M.P. “The thermal stability of diamond-like carbon”. *Diamond and Related Materials*, Vol.4, pp.191-199 (1995).

Wei, C., & Yen, J.Y. “Effect of film thickness and interlayer on the adhesion strength of diamond like carbon films on different substrates”. *Diamond and Related Materials*, Vol. 16, pp. 1325-1330 (2007).

Wu, W.Y., & Ting, J.M. “Growth and characteristics of carbon films with nano-sized metal particles”. *Thin Solid Films*, Vol. 420-421, pp. 166-171 (2002).

Yang, W.J., Choa, Y. H., & Sekino, T. “Thermal stability evaluation of diamond-like nanocomposite coatings”. *Thin Solid Films*, Vol. 434, pp. 49-54 (2003).

Zheng, X.H., Yang, F.E., & Chen, L. “Microstructure and mechanical properties of a-CNx films prepared by bias voltage assisted PLD with carbon nitride target”. *Surface and Coatings Technology*, Vol. 258, pp. 716-721 (2014).

Zhu, W., Stoner, B.R., & Williams, B.E. “Growth and characterization of diamond films on nondiamond substrates for electronic applications”. *Proceedings of the IEEE*, Vol. 79, pp. 621-646 (1991).

乙炔氣體的流量和鈦金屬的添加對於類鑽碳之機械與磨潤性質的影響

蘇演良 洪政豪 埃琳娜 Torskaya
高文顯 游展青

國立成功大學 機械工程所
國立虎尾科技大學 動力機械工程系
俄羅斯科學院Ishlisky力學研究所
建國科技大學 自動化工程學系

摘要

此論文研究了類鑽碳（DLC）、類鑽碳添加鈦金屬（DLC-Ti）和含氫類鑽碳添加鈦金屬（DLC-CH-Ti）等鍍層之機械與磨潤性質的影響。此研究使用非平衡磁控濺射法（CFUBMS）將上述鍍層濺鍍在高速鋼（SKH51）的基板上。輝光放電分光儀（GDS）的分析可以發現當加入乙炔氣體，鈦金屬的含量會降低。所有鍍層呈現出團簇的表面型態。X射線光電子光譜（XPS）分析也可以發現碳的sp^3鍵結的比例會隨著乙炔和鈦金屬的加入而增加。其中含氫類鑽碳添加鈦金屬的鍍層具有最佳的機械與磨潤性質，其磨耗率為0.09（$10^{-6}mm^3/Nm$），與Al_2O_3球對磨後的摩擦係數為0.11。這些結果都比其他鍍層來得佳，磨耗率甚至比原材還要低了約194倍，並且所有鍍層的耐腐蝕性也優於原材。